Neuron, Vol. 41, 737–744, March 4, 2004, Copyright ©2004 by Cell Press

Inactivation in HCN Channels Results from Reclosure of the Activation Gate: Desensitization to Voltage

Ki Soon Shin,[1,2] Chantal Maertens,[1,3] Catherine Proenza,[1] Brad S. Rothberg,[4] and Gary Yellen*
Department of Neurobiology
Harvard Medical School
220 Longwood Avenue
Boston, Massachusetts 02115

Summary

Hyperpolarization-activated HCN channels are modulated by direct binding of cyclic nucleotides. For HCN2 channels, cAMP shifts the voltage dependence for activation, with relatively little change in the maximal conductance. By contrast, in spHCN channels, cAMP relieves a rapid inactivation process and produces a large increase in maximum conductance. Our results suggest that these two effects of cAMP represent the same underlying process. We also find that spHCN inactivation occurs not by closure of a specialized inactivation gate, as for other voltage-dependent channels, but by reclosure of the same intracellular gate opened upon activation. Effectively, the activation gate exhibits a "desensitization to voltage," perhaps by slippage of the coupling between the voltage sensors and the gate. Differences in the initial coupling efficiency could allow cAMP to produce either the inactivation or the shift phenotype by strengthening effective coupling: a shift would naturally occur if coupling is already strong in the absence of cAMP.

Introduction

Hyperpolarization-activated cation channels contribute to rhythmic electrical activity in the heart and the brain (Brown et al., 1979; DiFrancesco, 1993; Pape, 1996; Pape and McCormick, 1989). These channels, known as I(f), I(h), or HCN channels, are modulated by direct binding of cyclic nucleotides to a site on the channel protein (DiFrancesco and Tortora, 1991). The presence of cAMP permits optimal activation of the channels at hyperpolarized voltages; when cAMP is removed, most mammalian HCN channels become more difficult to open due to a shift in the voltage dependence (Santoro et al., 1998; Ludwig et al., 1998). However, in the case of one HCN family member cloned from sea urchin (spHCN), removal of cAMP produces a large decrease in the maximum conductance that can be activated by hyperpolarization and reveals a rapid inactivation process (Gauss et al., 1998).

We have examined cAMP-influenced gating in both types of HCN channels. We find that the inactivation seen in the spHCN channels is not a unique feature of these channels: a latent inactivation process in the mammalian HCN2 channel can be revealed by a voltage prepulse experiment. Moreover, a single point mutation in the S6 gating region of spHCN can change the characteristic effect of cAMP on the channel to resemble the effect of cAMP on the mammalian HCN2 channel.

The classical models for inactivation of voltage-gated channels involve the closure of a specific "inactivation gate" that is distinct from the gate that opens upon activation (Yellen, 1998). For instance, Shaker Kv channels have a rapid "ball-and-chain" inactivation mechanism (N-type), and a slower C-type inactivation involving constriction of the selectivity filter. In contrast to these examples, the inactivation process in spHCN channels does not seem to arise from the action of a separate, specialized inactivation gate. Using pore blockers and a lock-open mutation to probe the gating process, we have found that inactivation and the corresponding reduced conductance seen when cAMP is removed appear to be a consequence of closure at the same intracellular gate that these channels use for voltage-controlled activation gating.

This picture of inactivation of spHCN channels suggests a different type of inactivation mechanism, which is closer to the current picture of desensitization in glutamate-gated ion channels (Sun et al., 2002). Hyperpolarization leads to voltage-sensor movement and channel opening—but then the weak linkage between the voltage sensor and the gate "fails," and the activation gate slips back to its shut position. Cyclic AMP may act either by opposing this slippage or by favoring the opening equilibrium. A natural consequence of this model for the effect of cAMP is that the two HCN channel phenotypes—cAMP-induced shift versus cAMP-controlled inactivation—can arise from the same basic gating scheme through quantitative differences in the slippage or opening equilibria.

Results

The Inactivation Phenotype of spHCN Can Be Converted to the Shift Phenotype of HCN2

The obvious difference in behavior between the sea urchin HCN clone (spHCN) and one of the mammalian HCNs (HCN2) is illustrated in Figure 1. In the presence of high levels of cAMP, the two channels behave quite similarly: they activate with hyperpolarizing voltage steps and remain open for the duration of the pulse. But in the absence of cAMP, a marked difference becomes apparent. The HCN2 channels primarily become a bit more difficult to open with voltage, as evidenced by a ~15 mV shift in the conductance-voltage (g-V) curve to more negative voltages. At negative voltages, though,

*Correspondence: gary_yellen@hms.harvard.edu
[1]These authors contributed equally to this work.
[2]Present address: Department of Anatomy and Neurobiology, College of Medicine, Kyunghee University, Dongdaemun-Gu, Hoegi-Dong 1, Seoul 130-701, Korea.
[3]Present address: Laboratory of Toxicology and Food Chemistry, Faculty of Pharmaceutical Sciences, KULeuven, E. Van Evenstraat 4, B-3000 Leuven, Belgium.
[4]Present address: Department of Physiology, University of Texas Health Science Center at San Antonio, 7703 Floyd Curl Drive, San Antonio, Texas 78229.

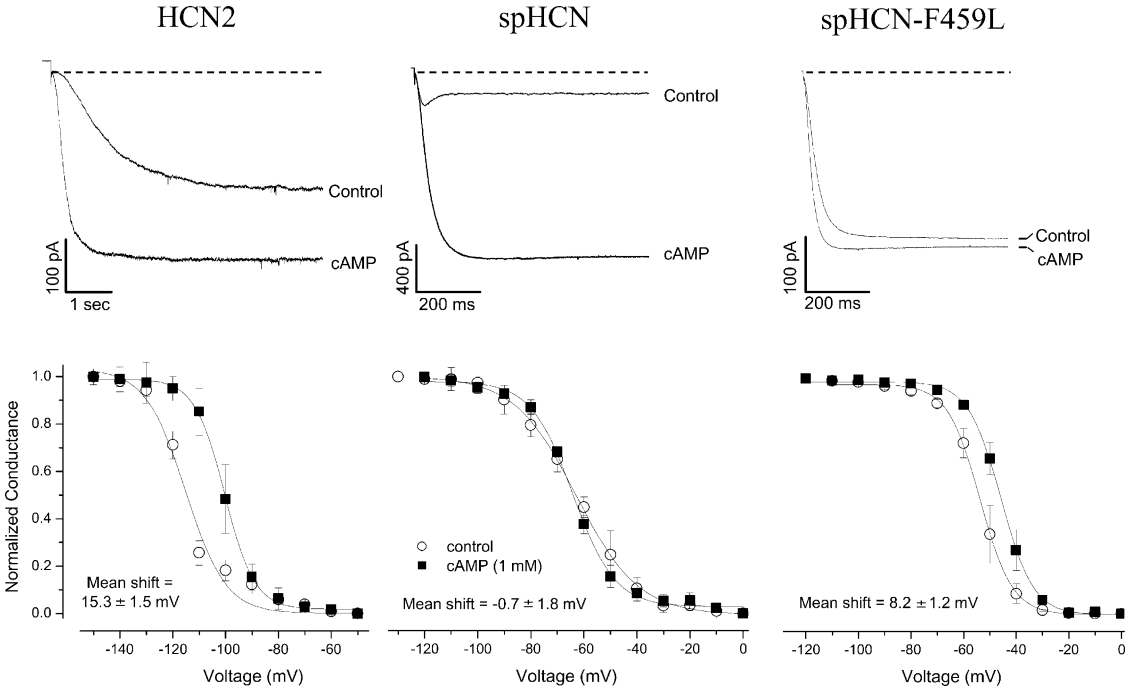

Figure 1. cAMP Effects on the Gating of HCN2, spHCN, spHCN-F459L

Top: Currents recorded for maximally activating voltage pulses in the presence or absence of cAMP in each channel, from inside-out patches. Bottom: Voltage dependence of channel activation. Tail current amplitudes at +60 mV were normalized to the maximal tail current. Solid line shows the best fit of the data to a Boltzmann function; normalized current = 1/[1 + exp (($V_{1/2}$ − V)/slope)], where V is voltage in mV and $V_{1/2}$ is the activation midpoint voltage. The activation midpoints were −115.9 ± 1.5 mV in the absence of cAMP and −100.7 ± 1.1 mV in the presence of 1 mM cAMP (n = 7) for HCN2, −62.9 ± 2.0 mV without and −63.6 ± 0.7 mV with cAMP (n = 4) for spHCN, and −53.3 ± 2.6 mV without and −45.1 ± 2.1 mV with cAMP (n = 6) for spHCN-459L. Position 459 is located in the S6 region of the spHCN channel. In an ungapped alignment of the P region and S6 region of the Kv and HCN channels, this position is homologous to the first proline of the conserved PVP sequence in the Kv channels. In spHCN and HCN1-4, this position is conserved as a phenylalanine (F). The S6 regions of the HCN channels have an overall ~70% sequence identity.

the maximal degree of activation is still substantial compared to that seen in the absence of cAMP (for maximally activating pulses, g-max is 76% ± 5% of that seen in the presence of cAMP, n = 3 for pulses > 5 s). By contrast, the spHCN channels show a marked decrease in steady-state conductance in the absence of cAMP. There is an early, small peak in the inward current, followed by rapid inactivation to a level that is far smaller than in the presence of cAMP, even at the most negative voltages.

The simplest description of each of these channels is that for HCN2 channels, cAMP produces a shift in the voltage dependence, making it easier for channels to open, while for spHCN channels, cAMP removes a rapid inactivation mechanism. (An alternative description that aids understanding of the gating is that *removal* of cAMP produces a voltage shift in the HCN2 channels, but produces inactivation in spHCN channels.) In both cases, cAMP increases the amount of HCN current, but on their face the mechanisms would appear to be quite different in the two cases.

In the course of our exploration of the S6 region of these channels, which lines the pore and acts as the voltage-controlled gate (Rothberg et al., 2002), we discovered a mutation of spHCN that essentially converts its behavior to that of the mammalian HCN2 channel. The gating of the spHCN-F459L mutant is shown at the right side of Figure 1. In the absence of cAMP, there is no longer any obvious inactivation, and the steady-state level of current at negative voltages is nearly as large as that seen in the presence of cAMP. Moreover, there is now a small but clear shift in the voltage dependence when cAMP is added (~8 mV), resembling the effect of cAMP on the HCN2 channel.

Conversion of the inactivating phenotype of spHCN to the shift phenotype of HCN2 involves not a loss of function but a change of function—459L channels have lost their prominent inactivation, but have also acquired the "shift" phenotype of HCN2. The ability to accomplish this conversion with a single point mutation in S6 argues strongly that the two channel types use the same fundamental mechanisms for gating, and that the different phenotypes represent differences "in the numbers"—that is, in the precise relationship between the energetics and kinetics of the different gating processes. This contention is supported by another series of experiments that revealed a "covert" inactivation process in the HCN2 channels.

Both HCN2 and spHCN Exhibit Prepulse-Induced Closed State Inactivation

In addition to observing the transient currents that arise from activation followed by inactivation, classical studies of channel inactivation rely on the application of long

voltage prepulses to discern the effect of inactivation on the subsequently activated currents (Hodgkin and Huxley, 1952). We applied this approach first to spHCN channels in the presence of cAMP, where no frank inactivation was apparent. We compared the currents evoked by an activating pulse directly from the holding potential (+10 mV) with those evoked after a prolonged (8 s) prepulse to −35 mV (Figure 2, top). Our initial expectation was that this subactivating prepulse would make subsequent activation faster, by pre-activating the channels from their deepest closed states into states more "ready to open" (Cole and Moore, 1960). The actual result was the opposite: the prepulses caused subsequent currents to activate more slowly, as though weakly activating prepulses put the channels into a more "difficult to activate" state—i.e., an inactivated state. Eventually the prepulsed channels "catch up" and reach the same steady-state level of current.

The effect of prepulses on spHCN activation was small but reproducible, and it did not result from drift or rundown, as it could be demonstrated by alternating between prepulse and nonprepulse trials.

A similar effect was seen for HCN2 channels (Figure 2, middle and bottom). As for the spHCN channels, the prepulse voltage was chosen to be at the foot of the g-V curve, so that little or no channel opening was produced during the prepulse. Application of a prepulse caused a reduction and slowing of the current activated during the subsequent test pulse (dotted traces in Figure 2). This effect was more striking for test pulses to voltages in the middle of the g-V curve; with more negative test pulses, the pre-inactivated currents eventually recover and produce the same level of current seen without a prepulse.

The effect appears to represent a form of closed-state inactivation, because it occurs following prepulses to voltages that do not produce significant voltage-dependent channel opening (Figure 3). Moreover, our impression is that the inactivation does not produce a complete incapacity of the channels to open, but rather it makes them more difficult to open: prepulse-inactivated channels just require larger hyperpolarizations to make them open. The small size of the effects and the tendency of the baseline g-V to shift from patch to patch, and with time during a recording, makes it difficult to characterize this behavior more quantitatively, but the qualitative features are robust and not an artifact of this variation. All of the channels studied here displayed some degree of prepulse inactivation even in the presence of cAMP, though the inactivation in cAMP usually appeared smaller and was easier to recover from at negative voltages (Figure 2).

The appearance of a prepulse-induced inactivation mechanism that is common to these various HCN channels supports the idea that the channels may produce their various phenotypes by the quantitatively different use of a shared mechanism.

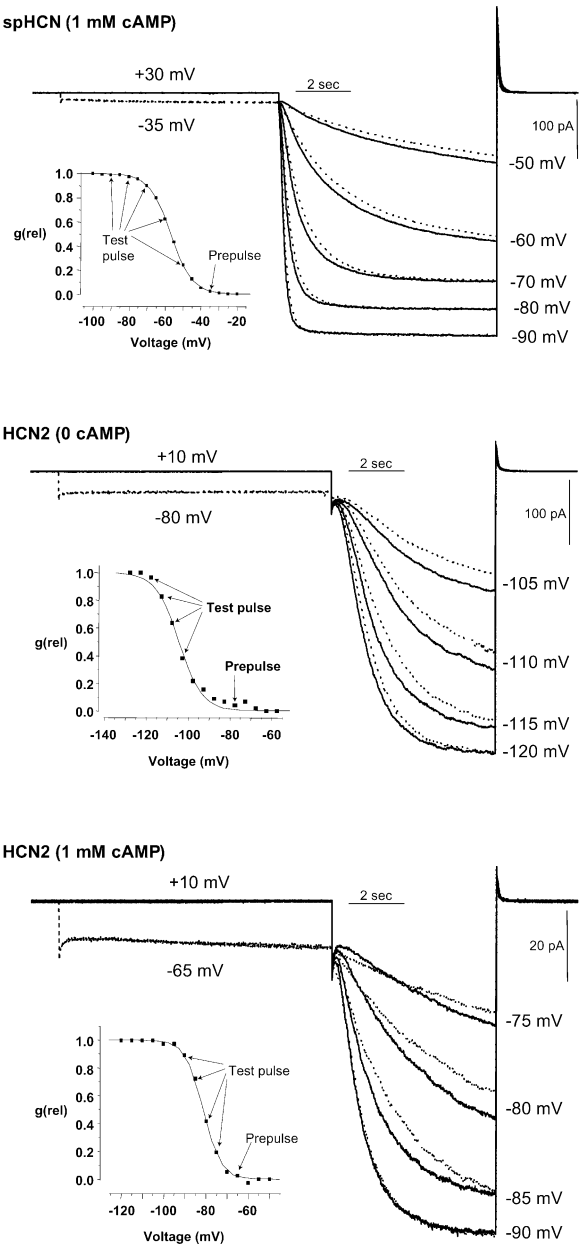

Figure 2. Prepulse-Induced Inactivation in spHCN and HCN2 Channels

Top: The effect of a 8 s prepulse to −35 mV on spHCN currents in the presence of cAMP, for test pulses from −50 to −90 mV. The currents are shown without the prepulse (solid lines) and with the prepulse (dotted lines). The inset shows the voltage dependence of activation for this experiment with an indication of the voltage pulses used in the main figure. Middle and bottom: Similar experiments on prepulse effects on HCN2 in the absence and presence of cAMP, for the voltages indicated. All these experiments were done in the high $[Ca^{2+}]_{out}$ solution (described in the Experimental Procedures), which shifts the voltage dependence of activation to more positive potentials.

In spHCN, Channel Closure by Removal of cAMP Involves an Intracellular Gate

What is the nature of the inactivation process in HCN channels? In K^+ channels, inactivation can involve the closure of specific inactivation gates, such as a ball-and-chain (tethered blocker) on the intracellular side or constriction of the selectivity filter at the extracellular side (Yellen, 1998). We used a pore blocker to learn what happens to pore accessibility in the clearest case of HCN inactivation, the inactivation of spHCN in the ab-

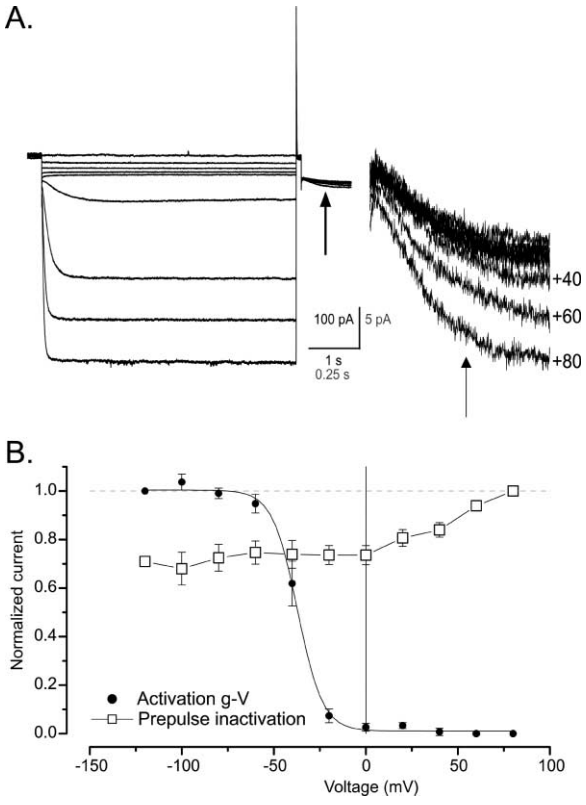

Figure 3. Prepulse Voltage Dependence of Inactivation in spHCN-F459L Channels

This experiment was performed in the absence of cAMP on spHCN-F459L channels because, of the channels we studied, only these have both large currents in the absence of cAMP and fast enough activation and deactivation gating to allow complete resetting of the activation process before there is much recovery from inactivation. (A) After steady-state activation and inactivation is achieved in a long prepulse (ranging from −120 to +80 mV), a brief depolarizing pulse was applied to +60 mV in order to deactivate channels activated in the prepulse (but not to permit much recovery from inactivation). The extent of the remaining inactivation is evaluated during a test pulse to −40 mV, at the time indicated by the arrow. A subsequent 1 s recovery pulse to −100 mV and a 15 s interpulse interval at +60 mV (not shown) minimized cumulative history effects on the patch. The inset at right shows the test pulse at an expanded scale. (B) Inactivation is induced even by prepulses to positive voltages where the open probability is very low. The average voltage dependence of activation (filled circles) is compared to the voltage dependence of inactivation (open squares) in the same patches using the protocol illustrated in (A) (n = 6). These experiments were done in the high $[Ca^{2+}]_{out}$ solution described in the Experimental Procedures.

sence of cAMP. Compared to the large conductance seen in the presence of cAMP, where is access to the pore restricted when the total conductance is reduced by removing cAMP?

To test whether access to the spHCN pore from the intracellular side was affected by removal of cAMP, we used the organic HCN channel blocker ZD7288. A previous study demonstrated that this blocker enters the pore from the intracellular side, and that this access is prevented by voltage-controlled gating (Rothberg et al., 2002; Shin et al., 2001). For wild-type spHCN channels, ZD7288 blockade is irreversible even with prolonged washout, so we used the rate of this irreversible blockade as an indication of the accessibility of the pore under different conditions. Figure 4A shows how we measured the ZD7288 entry in the constant presence of cAMP. Test pulses were applied every 4 s to measure the current. These test pulses were interrupted by brief (1 s) applications of ZD7288, done while channels were activated by a voltage step to −100 mV. Each drug application produced a strong reduction in the current measured in the subsequent test pulses. The overall inhibition is plotted as a function of the cumulative application time in Figure 4C; this shows a single exponential time course for inhibition in the presence of cAMP with a time constant of ~1.0 s for this experiment.

Because of the small size of the spHCN currents in the absence of cAMP, we used a slightly more complicated strategy to measure the inhibition rate. Before and after each application of ZD7288, test pulses in the presence of cAMP were used to assess the amount of inhibition. Cyclic AMP was washed out before each subsequent application of the blocker (and the duration of ZD7288 exposure was increased to 5 s because the inhibition was so slow). In the absence of cAMP, inhibition proceeded with a time constant of ~7.1 s in this experiment (Figure 4C).

On average, the inhibition rate for ZD7288 was reduced ~6-fold by removal of cAMP. This is comparable with the average change of ~8-fold in the inward current (Figure 4D). In other words, it appears that the channels become closed to blocker entry from the intracellular side when they are inactivated by removal of cAMP.

Trapping of ZD7288 in Channels Closed by cAMP Removal

Alternatively, the reduced rate of blockade we observed in the absence of cAMP might simply represent some sort of allosteric effect on the ZD7288 binding site. To investigate the mechanism of cAMP-induced gating further, we used a mutant spHCN channel that exhibits reversible blockade by ZD7288. As previously described, swapping three amino acids in S6 of spHCN channels with homologous mHCN1 residues (F456Y, L458M, I460V) makes the ZD7288 blockade reversible (Shin et al., 2001). This reversibly blocked mutant, named spHCN-χ3, showed normal cAMP gating behavior as well as normal voltage dependence like the wild-type channels (data not shown).

Using the spHCN-χ3 mutant, we tested whether ZD7288 could be trapped when channels are closed by removal of cAMP. First, a trapping experiment was done in the continuous presence of cAMP (Figure 5, top; Shin et al., 2001). Blocker was applied to the intracellular side of channels in the presence of cAMP at −110 mV to achieve steady-state block. Then the blocker was removed, and at the same time, the voltage was returned to +10 mV. After 40 s at this positive voltage where channels should be closed, a voltage step to −110 mV evoked only a slowly activating current (τ = ~3 s) whose time course reflects the slow unbinding of the blocker. The absence of normal rapidly activating currents indicates that the channels had remained blocked during the 40 s closing period. This result is consistent with the existence of the intracellular voltage-dependent activation gate in spHCN channels as previously described (Shin et al., 2001). In the second part of the experiment (Figure 5, bottom), after the blocker was applied as before, an

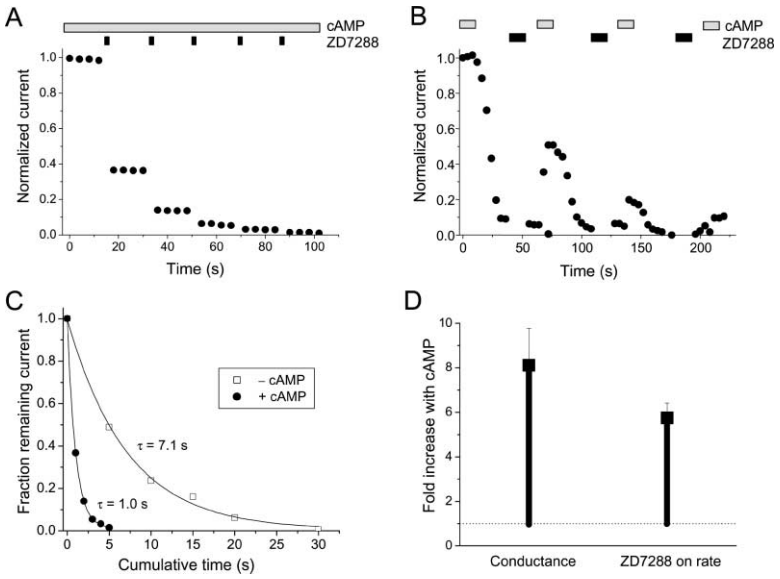

Figure 4. cAMP-Dependent ZD7288 Blockade of spHCN Channels

(A) In the constant presence of cAMP, ZD7288 (100 μM) was repeatedly applied to an inside-out patch for 1 s at −100 mV at each time point indicated by the black bars. Dots indicate the steady-state current in response to an activating voltage step to −120 mV applied every 4 s between blocker applications.

(B) In the absence of cAMP, ZD7288 (100 μM) was repeatedly applied to an inside-out patch for 5 s at −100 mV. Brief applications of cAMP (100 μM) were used to assess the reduction in current.

(C) Fractional remaining currents after each application of ZD7288 (100 μM) were measured either in the presence or in the absence of cAMP as shown in (A) and (B) and plotted against cumulative treatment time. The rate constant for the irreversible block was calculated from a time constant of a mono-exponential fit to the data.

(D) cAMP-induced difference in rate of irreversible blockade was comparable to cAMP-induced difference in conductance. The rates were measured as described in (C) with 100 μM ZD7288. For comparison, the fold-increase in conductance by cAMP is shown. All individual points give the mean and standard error of at least three determinations. Rates were 0.19 ± 0.03 s^{-1} in the absence of cAMP and 1.11 ± 0.07 s^{-1} in the presence of cAMP.

8 s "recovery" step to −110 mV was applied in the absence of cAMP. During this period, the channels should be mostly in the inactivated state. To test for recovery, a subsequent activating voltage step to −110 mV was applied again in the presence of cAMP. The slow activation of currents during this second voltage step ($\tau = \sim 3$ s), with only a tiny rapid activation component, suggests that the blocker remained trapped in the inactivated channels. The result further supports the idea that inactivation/closure of spHCN channels by removal of cAMP is due to closure of a gate that is located at the intracellular entrance to the pore.

A Metal-Induced Lock-Open Effect in a spHCN Mutant Prevents Closure Both by Voltage and by Removal of cAMP

It appears that both voltage-controlled activation gating and cAMP-controlled inactivation gating depend on an intracellular gate, but what is the relationship between the two gating processes? One possibility is that opening of the activation gate is followed by closure of a separate gate, like the N-type inactivation gate (ball-and-chain) of Shaker Kv channels (Hoshi et al., 1990). Alternatively, HCN inactivation might result from reclosure of the *same* gate that opens upon activation. Evidence to favor this latter idea came from experiments on a mutant spHCN channel with two cysteines introduced into each subunit at positions 462 and 466 in the S6 region. We found previously that the 466C mutant channels can be "locked open" by low concentrations of Cd^{2+}, so that deactivation at positive voltages is substantially slowed (Rothberg et al., 2003). This effect is even stronger when the native histidine at position 462 is replaced by a cysteine (Rothberg et al., 2003); the two cysteines together produce a Cd^{2+}-induced lock-open effect that takes many minutes to reverse. Our previous

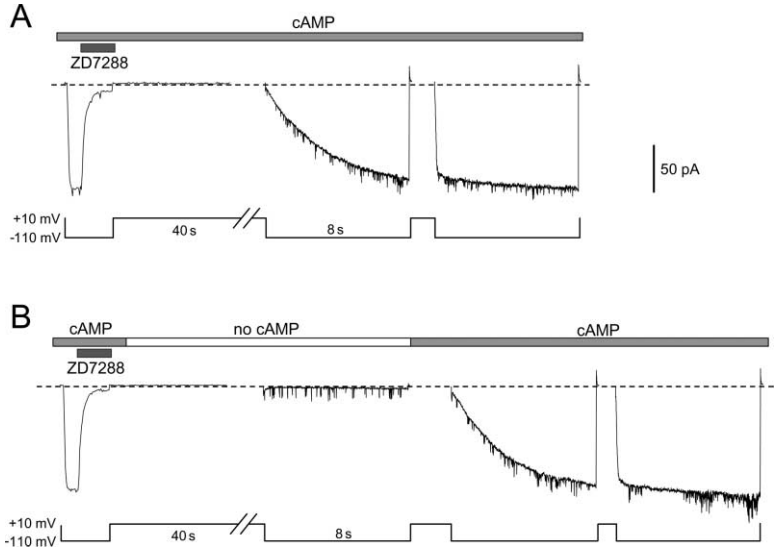

Figure 5. Trapping of ZD7288 in Inactivated Channels in the Absence of cAMP in Reversibly Blocked spHCN-χ3 Mutant Channels

(A) ZD7288 (100 μM) was applied to an inside-out patch for 1 s at −110 mV (black bars), in the constant presence of cAMP (100 μM). After closing channels at +10 mV, the blocker was washed away. Recovery was then observed during two 8 s test pulses to −110 mV.

(B) Blocker trapping and recovery was again examined, except cAMP was removed during the first of three 8 s recovery pulses to −110 mV. There was little recovery during this hyperpolarizing step in the absence of cAMP, but subsequent recovery in the presence of cAMP (with $\tau \sim 3$ s) was very similar to that obtained in (A).

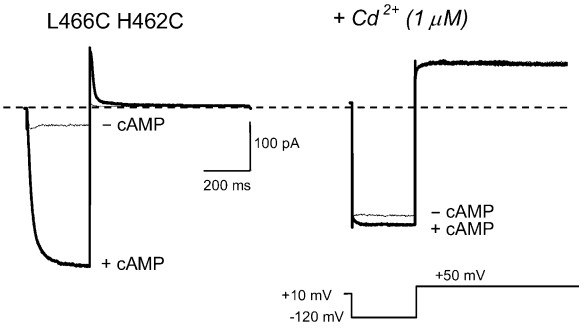

Figure 6. A Lock-Open Effect of Cd^{2+} on spHCN-462C-466C Channel Prevents Closure by Voltage or by Removal of cAMP

Left: The mutant channel shows a normal spHCN-type response to cAMP (100 μM). Right: In the presence of 1 μM Cd^{2+}, the channels are locked open: there is no deactivation of channels at the tail voltage of +50 mV, and there is only a tiny reduction of inward current in the absence of cAMP.

experiments on the S6 mutants were done in the constant presence of cAMP, and we concluded that Cd^{2+} binding was capable of opposing or preventing the voltage-controlled closure of the channels. We now investigated the effect of Cd^{2+} on the cAMP-controlled gating.

With no Cd^{2+} present, the double mutant H462C L466C showed the normal pattern of cAMP effect: in the absence of cAMP, the current was small and inactivating (Figure 6, left). After application of 1 μM Cd^{2+}, the channels were locked open, with the time-dependent activation at negative voltage almost eliminated (Figure 6, right). Almost all the current was apparent as an instantaneous jump upon changing the voltage, and there was no deactivation apparent in 0.5 s at +50 mV. With Cd^{2+}, the current is nearly identical in the presence and absence of cAMP (there is a small time-dependent current increase in cAMP that is not seen in the absence of cAMP, but there is no difference in the tail currents). The maximum locked open current is ~25% smaller than the maximum current with cAMP and no Cd^{2+}, as is seen for all of the L466C lock-open effects (Rothberg et al., 2003). On the other hand, Cd^{2+} substantially *increases* the current seen in the absence of cAMP.

The lock-open effect eliminates the inactivation/inhibition caused by removal of cAMP. This is contrary to the relationship seen for Shaker Kv channels between a similar lock-open effect and the N-type (ball-and-chain) inactivation mechanism: there, locking the activation gate open enhances the ability of the inactivation peptide to inhibit the channel (S.M. Webster and G.Y., unpublished data). Our interpretation is that the Cd^{2+} binding to this spHCN mutant prevents closure not just of the voltage-controlled gate, but also of the cAMP-controlled gate. The simplest explanation is that voltage- and cAMP-controlled gating use the same gate.

Discussion

The Various Effects of cAMP on Inactivation and Voltage Dependence Can Be Explained by Simple Quantitative Differences in Gating Equilibria

The ability of a single point mutation to change the cAMP gating phenotype of spHCN channels to resemble that of HCN2, together with the demonstration of covert inactivation in the HCN2 channels, indicates an essential similarity between the gating machinery of these two channels. How could this gating machinery give rise to the two cAMP phenotypes, on the one hand a relief of inactivation, and on the other a shift in the voltage dependence of gating? A simplified model of HCN gating, which includes an inactivated state accessible from the closed state, is capable of producing these two alternative behaviors in a straightforward way.

A simple model that incorporates voltage-dependent channel opening and inactivation from both closed and open states is shown here.

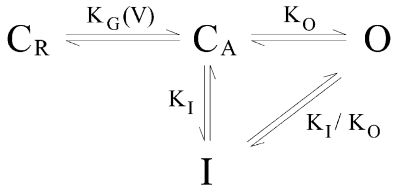

In this model, the resting closed state (at positive voltages) is C_R. Hyperpolarization causes entry first into the activated closed state C_A and then into the open state. If the $C_A \leftrightarrow O$ steps are fast compared to the $C_A \leftrightarrow I$ and $O \leftrightarrow I$ steps, then hyperpolarization can lead to transient opening that gives way to steady-state inactivation. The overall open probability in the steady-state, at limiting negative voltages, is determined by the values of K_O and K_I, with $p_{OPEN} = K_O/(1 + K_O + K_I)$.

In principle, the cAMP-induced increase in open probability seen for spHCN channels (and the absence of transient inactivation) could be explained by cAMP producing either a decrease in the equilibrium constant for inactivation (K_I) or an increase in the final opening equilibrium (K_O). In either case, the steady-state occupancy of the open state would increase substantially. What about the shift phenotype seen for the HCN2 channels? Suppose that the only difference between HCN2 channels and spHCN channels is in the final opening equilibrium (K_O). Qualitatively, if K_O is relatively small (less than or near one), then the main effect of increasing it is to raise the limiting open probability, but if the value is large to begin with, then increasing it produces mainly a shift in the voltage dependence that favors opening. For example, suppose that for both channels, $K_I = 5$, but that for spHCN channels, cAMP changes K_O from 0.1 to 2.5, while for HCN2 channels, cAMP changes K_O from 10 to 250. With these values, the effect of cAMP on the spHCN channels is mainly a change in limiting open probability (~5×), with a negligible voltage shift (~2 mV); but the effect on HCN2 would be a 1.6× increase in limiting open probability with a substantial voltage shift (~19 mV; these numbers assume a steepness of e-fold per 7 mV for the voltage-dependent K_G step; see Supplemental Data at http://www.neuron.org/cgi/content/full/41/5/737/DC1). A cAMP-induced change in K_O would allow the two phenotypes to be explained naturally by a single effect of cAMP, whereas allowing cAMP to change K_I alone would relieve inactivation but would produce a voltage shift in the wrong direction.

This basic model for the gating can explain the essential properties of cAMP-induced gating qualitatively and

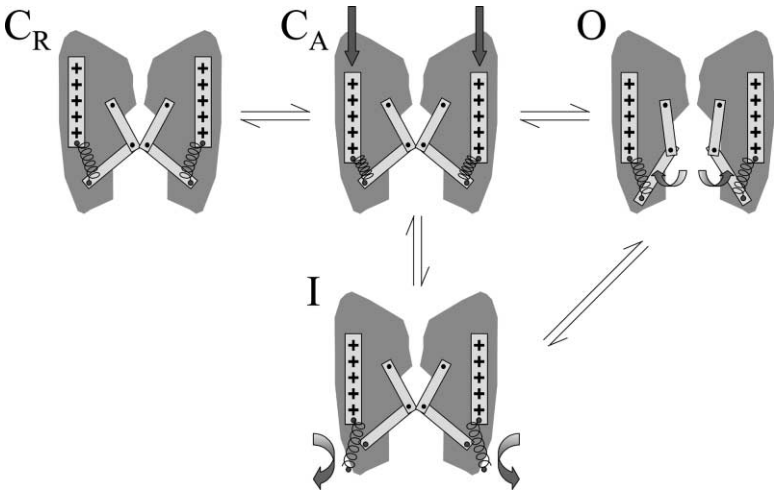

Figure 7. Cartoon of HCN Inactivation as Slippage of the Coupling between Voltage Sensor and Gate: "Desensitization to Voltage"

On hyperpolarization, the voltage sensors (transmembrane segments with multiple +ve charges) move inward (C_R to C_A). With activation of enough voltage sensors, the channels open their intracellular gate (O); but if the coupling between voltage sensors and the gate (depicted here as a spring) should slip, the channel inactivates (I). If only one or two sensors slip, it may still be possible to activate the channels with the remaining voltage sensors, but with more difficulty (as seen in prepulse-induced inactivation).

nearly quantitatively, though of course to capture the complex kinetics of HCN currents requires a model with many more states. We expect that a good framework for a more complex model will be the allosteric approach used by Horrigan and Aldrich (2002) to explain the coordinate effects of voltage and Ca^{2+} on the gating of BK channels. The more complete treatment includes multiple activated but closed (C_A) states, with different numbers of activated voltage sensors, allowing it to handle certain phenomena much better than the oversimplified four-state model. Specifically, it can explain the induction of significant inactivation at voltages that produce little opening (Figure 3), and the recovery from inactivation at the most negative voltages (Figure 2).

The persistence of prepulse-induced inactivation in the presence of cAMP (Figure 2) is compatible with the idea that cAMP does not eliminate the inactivated state, but instead favors the $C_A \rightarrow O$ equilibrium. For small prepulse steps, the $C_A \rightarrow O$ equilibrium (which is effectively voltage dependent in the more complex model) is well below the maximum value achieved at very negative voltages and thus would permit inactivation to occur, with subsequent recovery during subsequent, strongly activating steps.

Inactivation as Reclosure of the Activation Gate

For spHCN channels, the effect of cAMP on access of ZD7288 between the intracellular bathing solution and the binding site within the pore is strong evidence that cAMP-controlled gating involves an intracellular gate. The ability of the 462C-466C Cd^{2+} lock-open effect to prevent both voltage-controlled closure and cAMP-controlled closure of the pore gives the strong impression that voltage and cAMP are controlling the *same* intracellular gate.

Removal of cAMP produces a large reduction in the current through spHCN channels: the initial rising phase of the current is similar to that seen in the presence of cAMP, but then the current declines ("inactivates") to a much smaller steady-state level. Apparently this "inactivation" is due to a closure of the intracellular *activation* gate. (We attribute the rapid inactivation and the steady-state reduction to the same process, but it is difficult to test this experimentally because the transient peak is too brief to allow us to use ZD binding as a tool.)

What does it mean to say that inactivation is due to a closure of the intracellular activation gate? Apparently a hyperpolarizing voltage stimulus causes the activation gate to open, but then in spite of the maintained stimulus, it slips shut again. In some sense, the channel "desensitizes" to the voltage stimulus. We envision this as a temporary uncoupling between the voltage sensors and the gate: though the voltage sensors remain in their hyperpolarized activated position, somehow the linkage that couples these sensors to the gate comes undone and allows the gate to close (see Figure 7). In terms of our simple model described above, the activated-but-not-open C_A state has an energetic tension between the voltage sensors (which "want" the gate to open) and the gate (which remains closed). This tension can be resolved either by opening, so that the two parts of the protein "agree" with each other, or by uncoupling (to yield the inactivated state I). Binding of cAMP increases the forward equilibrium constant for opening (K_O), and by reducing the occupancy of C_A, it reduces the tension that leads to inactivation.

The model we propose of "desensitization to voltage" is very different from the traditional view of inactivation processes in voltage-gated channels, invoking the action of specialized inactivation gates. On the other hand, it is analogous to the process of desensitization in ligand-gated channels, a process that is becoming very well understood at a structural level for ionotropic glutamate receptors (Sun et al., 2002). In that case, it appears that glutamate-induced closure of the clamshell-shaped binding domain provides the energy for the channel to open, but that this also produces stress at the dimer interface between binding domains. Rupture at the dimer interface leads to desensitization. Although the details are certain to be different, the glutamate receptors demonstrate this basic theme of desensitization through slippage or uncoupling.

We suspect that this process of inactivation through desensitization to voltage, described here for the sea urchin spHCN channel, is not unique to these channels and is likely to occur in other members of the voltage-gated channel superfamily.

Experimental Procedures

Expression of Recombinant HCN Channels

Channels were transiently expressed in Human Embryonic Kidney 293 cells (HEK 293; American Type Culture Collection) as described previously (Shin et al., 2001). Cells were cotransfected with the πH3-CD8 plasmid (Seed and Aruffo, 1987), which expresses the α subunit of the human CD8 lymphocyte antigen. Cells expressing the CD8 antigen were identified by decoration with antibody-coated beads (Jurman et al., 1994). spHCN channels contained the M349I mutation to increase functional expression levels (Shin et al., 2001). The F459L point mutation was introduced by PCR and confirmed by sequencing.

Solutions and Electrophysiological Recordings

All experiments were performed with excised inside-out patches (Hamill et al., 1981) from identified transfected cells 1–2 days after transfection. Experiments were done at room temperature (22°C–24°C). Currents were low-pass filtered at 1–2 kHz and digitized at 5–50 kHz. Unless otherwise specified, all experiments were performed with a bath solution of (in mM) 160 KCl, 1 $MgCl_2$, 10 HEPES, 1 EGTA (pH 7.4) with KOH. The pipette solution (extracellular) was the same, but without EGTA. For the experiments on prepulse inactivation, we used a high $[Ca^{2+}]_{out}$ solution to shift activation to less negative voltages (Malcolm et al., 2003). Bath solution: 140 KCl, 1 EGTA, 0.5 $MgCl_2$, 10 HEPES, 60 mannitol (pH 7.4) with KOH; pipette solution: 140 KCl, 20 $CaCl_2$, 0.5 $MgCl_2$, 10 HEPES (pH 7.4) with KOH.

Acknowledgments

We are grateful to the members of the Yellen laboratory for helpful discussions and to Tatiana Abramson for her expert help with transfections. We thank Dr. U.B. Kaupp for the spHCN clone and Dr. M. Biel for the HCN2 clone. The work was supported by grants from the NIH-NHLBI (HL 70320 to G.Y.), a McKnight Investigator Award (to G.Y.), fellowships from the NIH-NHLBI (HL71365 to C.P.), and the Belgian American Educational Foundation (to C.M.).

Received: October 30, 2003
Revised: January 5, 2004
Accepted: January 6, 2004
Published: March 3, 2004

References

Brown, H.F., DiFrancesco, D., and Noble, S.J. (1979). How does adrenaline accelerate the heart? Nature *280*, 235–236.

Cole, K.S., and Moore, J.W. (1960). Potassium ion current in the squid giant axon: dynamic characteristic. Biophys. J. *1*, 1–14.

DiFrancesco, D. (1993). Pacemaker mechanisms in cardiac tissue. Annu. Rev. Physiol. *55*, 455–472.

DiFrancesco, D., and Tortora, P. (1991). Direct activation of cardiac pacemaker channels by intracellular cyclic AMP. Nature *351*, 145–147.

Gauss, R., Seifert, R., and Kaupp, U.B. (1998). Molecular identification of a hyperpolarization-activated channel in sea urchin sperm. Nature *393*, 583–587.

Hamill, O.P., Marty, A., Neher, E., Sakmann, B., and Sigworth, F.J. (1981). Improved patch-clamp techniques for high-resolution current recording from cells and cell-free membrane patches. Pflugers Arch. *391*, 85–100.

Hodgkin, A.L., and Huxley, A.F. (1952). The dual effect of membrane potential on sodium conductance in the giant axon of *Loligo*. J. Physiol. *116*, 497–506.

Horrigan, F.T., and Aldrich, R.W. (2002). Coupling between voltage sensor activation, Ca^{2+} binding and channel opening in large conductance (BK) potassium channels. J. Gen. Physiol. *120*, 267–305.

Hoshi, T., Zagotta, W.N., and Aldrich, R.W. (1990). Biophysical and molecular mechanisms of Shaker potassium channel inactivation. Science *250*, 533–538.

Jurman, M.E., Boland, L.M., Liu, Y., and Yellen, G. (1994). Visual identification of individual transfected cells for electrophysiology using antibody-coated beads. Biotechniques *17*, 876–881.

Ludwig, A., Zong, X., Jeglitsch, M., Hofmann, F., and Biel, M. (1998). A family of hyperpolarization-activated mammalian cation channels. Nature *393*, 587–591.

Malcolm, A.T., Kourennyi, D.E., and Barnes, S. (2003). Protons and calcium alter gating of the hyperpolarization-activated cation current (I(h)) in rod photoreceptors. Biochim. Biophys. Acta *1609*, 183–192.

Pape, H.C. (1996). Queer current and pacemaker: the hyperpolarization-activated cation current in neurons. Annu. Rev. Physiol. *58*, 299–327.

Pape, H.C., and McCormick, D.A. (1989). Noradrenaline and serotonin selectively modulate thalamic burst firing by enhancing a hyperpolarization-activated cation current. Nature *340*, 715–718.

Rothberg, B.S., Shin, K.S., Phale, P.S., and Yellen, G. (2002). Voltage-controlled gating at the intracellular entrance to a hyperpolarization-activated cation channel. J. Gen. Physiol. *119*, 83–91.

Rothberg, B.S., Shin, K.S., and Yellen, G. (2003). Movements near the gate of a hyperpolarization-activated cation channel. J. Gen. Physiol. *122*, 501–510.

Santoro, B., Liu, D.T., Yao, H., Bartsch, D., Kandel, E.R., Siegelbaum, S.A., and Tibbs, G.R. (1998). Identification of a gene encoding a hyperpolarization-activated pacemaker channel of brain. Cell *93*, 717–729.

Seed, B., and Aruffo, A. (1987). Molecular cloning of the CD2 antigen, the T-cell erythrocyte receptor, by a rapid immunoselection procedure. Proc. Natl. Acad. Sci. USA *84*, 3365–3369.

Shin, K.S., Rothberg, B.S., and Yellen, G. (2001). Blocker state dependence and trapping in hyperpolarization-activated cation channels: evidence for an intracellular activation gate. J. Gen. Physiol. *117*, 91–101.

Sun, Y., Olson, R., Horning, M., Armstrong, N., Mayer, M., and Gouaux, E. (2002). Mechanism of glutamate receptor desensitization. Nature *417*, 245–253.

Yellen, G. (1998). The moving parts of voltage-gated ion channels. Q. Rev. Biophys. *31*, 239–295.